

Mechanical and Physical Characterization of Polyoxymethylene Processed by High-Velocity Compaction

D. Jauffrès,¹ O. Lame,¹ G. Vigier,¹ F. Doré,² C. Chervin³

¹MATERiaux: Ingénierie et Science (MATEIS), INSA-Lyon, CNRS UMR5510, Bât. B. Pascal 7 Avenue Jean Capelle, F-69621 Villeurbanne Cedex, France

²Centre Technique des Industries Mécaniques (CETIM), 7 Rue de la Presse, BP802, F-42952 Saint Etienne Cedex 9, France

³DuPont de Nemours International S.A., 2 Chemin du Pavillon, BP50, CH-1218 Le Grand Saconnex, Switzerland

Received 18 December 2006; accepted 19 January 2007

DOI 10.1002/app.26231

Published online 26 June 2007 in Wiley InterScience (www.interscience.wiley.com).

ABSTRACT: Conventional polymer processes, such as injection and extrusion, require the melting of the polymer. High-velocity compaction (HVC) allows the processing of polymer powders via sintering without the need of a melting stage. It opens up a new horizon for polymers that have processing issues linked to the melting stage. Because of chemical degradation above the melting point and significant shrinkage, the injection of semicrystalline polymer polyoxymethylene (POM) is often problematic. Nascent, highly crystalline POM powder has been successfully processed by HVC, and this process appears to be an interesting alternative to injection for certain applications. POM

processed by HVC has a remarkably high stiffness but is brittle. A microstructural investigation, involving differential scanning calorimetry experiments and scanning electron microscopy, has been conducted to explain these unusual mechanical properties. It appears that in POM processed by HVC, the stiffness is due to particularly high crystallinity, and brittleness is intrinsic to nascent POM powder. © 2007 Wiley Periodicals, Inc. *J Appl Polym Sci* 106: 488–497, 2007

Key words: mechanical properties; morphology; processing; sintering

INTRODUCTION

In the polymer industry, conventional processes (principally injection and extrusion) involve polymer melting. Consequently, these processes have several drawbacks:¹

- Risks of polymer chemical degradation induced by high temperatures.
- Significant shrinkage and cavity formation during the crystallization of semicrystalline polymers due to density differences between the crystal and amorphous phases.
- Processing difficulties for viscous polymers.
- Significant energy cost to melt the polymer.

Furthermore, mechanical property improvements in a material are limited by conventional process requirements, such as a low viscosity and low density variations. Indeed, better properties can be obtained by increases in the polymer molecular weight or the addition of fillers. Unfortunately, this increases the viscosity drastically and thus leads to

processing difficulties. A high crystallinity also leads to improved mechanical properties but induces high shrinkage and cavity formation during cooling.

Alternative processes inspired by powder metallurgy² have been developed for high-viscosity polymers: polytetrafluoroethylene cold compaction followed by sintering^{3,4} and ultrahigh-molecular-weight polyethylene compression molding^{5,6} are successfully used industrially. They offer satisfactory solutions to viscosity problems, but applications are limited because the processing is long (several hours) and expensive.

Polyoxymethylene (POM) is a semicrystalline thermoplastic polymer with valuable mechanical properties (Young's modulus = 3 GPa, yield stress = 70 MPa⁷) and good tribological properties that make it particularly suitable for industrial applications such as gear wheels and pinions, fixture gears, and ski bindings. However, POM injection is difficult and requires specific expertise. Indeed, its high crystallinity degree (60–90%) and density difference between the crystal (1.49 g/cm³) and amorphous phases (1.21 g/cm³) induce significant shrinkage and cavity formation.⁸ Consequently, its applications, especially regarding part thickness that should generally not exceed 10 mm,⁹ are limited. POM is also strongly sensitive to chemical degradation above its melting temperature (~178°C). The degradation becomes signifi-

Correspondence to: O. Lame (olivier.lame@insa-lyon.fr).

cant (gas formaldehyde outburst) above 230°C for the stabilized POM used in conventional processing.¹⁰

In this study, we consider the production of POM parts without significant melting to avoid the aforementioned processing difficulties. The high-velocity compaction (HVC) press developed at CETIM (Technical Center, St Etienne, France)¹¹ allows the processing of polymers below their melting temperature by applying several high-energy impacts to a powder-filled die to sinter the powder. The purpose of this article is to compare the mechanical and physical properties of conventionally processed POM and high-velocity-compaction polyoxymethylene (POM-HVC). In addition, a sintering mechanism is proposed.

EXPERIMENTAL

Nascent POM powder

DuPont Delrin POM (Le Grand Saconnex, Switzerland) was used in this study. It is produced by solution polymerization, which leads to spherical nascent particles 50–200 μm in size. Crystallization occurs simultaneously with polymerization, imparting to this powder an exceptional crystallinity degree ($\sim 90\%$) that is really higher than the crystallinity degree of POM crystallized from the melt ($\sim 70\%$). This nascent powder is generally stabilized and extruded to form pellets for conventional processing. We decided to work directly with the nascent powder rather than grinding pellets. The nascent powder exhibits two main advantages: its size is compatible with sintering (50–200 μm), and its crystallinity is very high. On the other hand, the nascent powder is not stabilized, and chemical degradation occurs once it has melted.

The POM glass transition occurs near -70°C , and its crystal relaxation (usually called the α_c relaxation) occurs between 100 and 120°C at 1 Hz. POM melts at 178°C .^{7,12–14}

Delrin grade 500 with a number-average molecular weight of = 45,000 g/mol (number average) was used in this study.

HVC process

The HVC process is carried out in three main steps (Fig. 1): powder filling (step A), compaction impacts (step B), and ejection (step C). Tools are heated at the chosen process temperature. First, the die is filled with a few dozen grams of the polymer powder (step A). To have a homogeneous temperature, the powder is heated for 20 min at the process temperature before the powder filling.

After this first step, the upper punch is placed on the powder, and a static precompaction is applied at 60 MPa. Then, the HVC hammer impacts the upper punch several times at the frequency of one impact

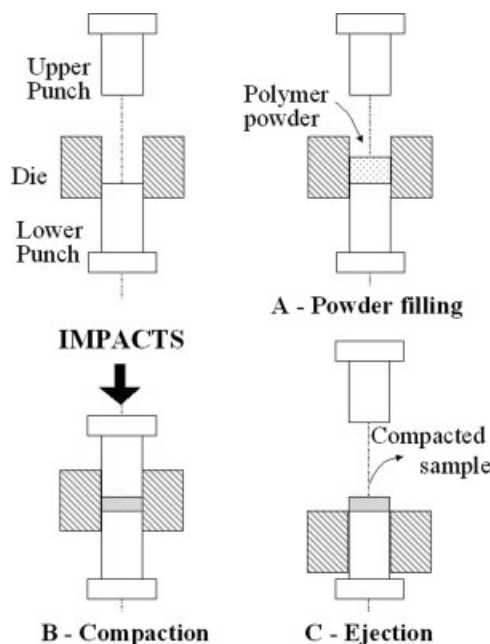


Figure 1 Three steps of HVC compaction.

per second (step B).¹¹ The HVC hammer kinetic energy and the number of impacts are controlled. Finally, the die descent provokes the sample ejection (step C). The sample shape is a disc with a thickness of a few millimeters and a diameter of 50 mm.

Choice of the parameters

The processing temperatures should be chosen under the POM melting temperature to keep the polymer in the solid state. However, the polymer must be processed above its crystal mechanical relaxation temperature (~ 100 – 120°C) to enhance large crystal deformation and generate enough mobility for sintering. As a result, three processing temperatures were chosen between the crystal relaxation and the melting point: 120, 130, and 140°C .

The impact energy was fixed at 1 kJ (maximum value limited for technological reasons). It was not possible to increase this value. Five to one hundred impacts were performed to obtain different total compaction energies (HVC hammer impact energy multiplied by the number of impacts). The number of impacts was limited to 100 to keep a reasonable processing time.

Actually, the total compaction energy does not correspond to the energy really brought to the powder. Indeed, there are viscoelastic rebounds, which propagate in the tools and the press, dissipating a significant part of the energy. The parameters chosen for the HVC experiments are listed in Table I. The HVC samples have been classified into three categories according to the total energy (low-, medium-, and high-energy HVC).

TABLE I
Processing Parameters

| Temperature (°C) | Total energy (kJ) | HVC |
|------------------|-------------------|--------|
| 120 | 5 | Low |
| 120 | 10 | |
| 130 | 5 | |
| 140 | 4 | |
| 140 | 8 | |
| 120 | 30 | Medium |
| 130 | 20 | |
| 130 | 30 | |
| 130 | 30 | |
| 130 | 40 | |
| 140 | 20 | High |
| 140 | 50 | |
| 140 | 50 | |
| 140 | 100 | |

Characterization methods

The following methods were used:

- The material crystallinity degree was measured by differential scanning calorimetry (DSC).
- The density was measured to evaluate the porosity.
- Dynamic mechanical analysis (DMA) was performed to provide information both on the mechanical relaxations and on the mechanical properties at small strains.
- Mechanical characterization until rupture was performed with bending and compressive tests.
- Low-voltage scanning electron microscopy (LVSEM) was performed on bending test fracture surfaces.

DSC

DSC characterizes polymer phase transformations, particularly the melting of the crystalline part. Enthalpy variations versus the time and temperature were obtained from DSC during controlled heating.

A PerkinElmer DSC Pyris (Waltham, MA) was used with a temperature ramp of 10°C/min from 100 to 200°C. A mass of 5 ± 1 mg was chosen, and precautions were taken to ensure a stable sample specific surface to keep a constant thermal transfer coefficient.

The melting temperature of the sample, its crystal weight fraction (X_c), and its crystal volume fraction (Φ_c) were obtained from DSC curves:

$$X_c = \frac{\Delta H_m}{\Delta H_{m0}} \quad (1)$$

$$\Phi_c = X_c \cdot \frac{\rho_a}{\rho_c - X_c \cdot (\rho_c - \rho_a)} \quad (2)$$

where ΔH_m is the sample melting enthalpy (corresponding to the melting peak area), ΔH_{m0} is the full

crystalline sample melting enthalpy (250 J/g by Wunderlich⁸), ρ_c is the density of the crystal phase, and ρ_a is the density of the amorphous phase.

From the Gibbs–Thomson equation, the melting temperature (T_m) can be related to the crystal lamellar thickness (l_c) and surface energy (σ):

$$T_m = T_m^0 \cdot \left(1 - \frac{2 \cdot \sigma}{\Delta H_{m0} \cdot l_c} \right) \quad (3)$$

where T_m^0 is the melting temperature of the infinite-size crystal.¹⁵

Density measurements

The densities were obtained by the weighing of the POM-HVC samples and the determination of their volume through the intermediary of Archimedes force. This method led to a precision of 5×10^{-3} .

DMA

DMA provides the complex modulus versus the temperature and allows the study of the mechanical relaxations. Parallel-piped samples (30 mm × 3 mm × 1 mm) were machined and then tested in a torsion pendulum as a function of temperature. A frequency of 1 Hz and a heating rate of 1°C/min were used. The shear modulus and loss angle were computed from the integration of the stress and strain functions.

Mechanical testing

Three-point-bending tests and compressive tests were carried out. The bending test was preferred to the tensile test for its simplicity and good accuracy for the modulus measurement. In addition, compressive tests were performed to allow better characterization of the plasticity behavior.

The three-point-bending-test samples were 3 mm thick, 6 mm wide, and 30 mm long. The distance between the two external contacts was 25 mm. The strain rate was $5 \times 10^{-4} \text{ s}^{-1}$. The stress and strain were calculated from force and deflection measurements, in the small deformation hypothesis, according to ASTM D 790.¹⁶

Compressive tests were carried out with 10-mm-high parallel-piped samples (6 mm × 6 mm section). The strain rate was $2 \times 10^{-3} \text{ s}^{-1}$.

LVSEM

The microstructure was observed by LVSEM on failure surfaces obtained after bending tests with an FEI XL-30 ESEM FEG (Hillsboro, OR). The use of a low

accelerating voltage (between 0.8 and 1.2 kV) allowed the observation of nonconductive samples without a metal coating, and thus the original sample surface characteristics were preserved.

RESULTS

Microstructure characterization (DSC)

DSC curves for nascent powder polyoxymethylene (POM-N), compression-molded polyoxymethylene (POM-CM), and POM-HVC are presented in Figure 2.

As the POM-HVC curves do not vary significantly with the process parameters (energy and temperature), only one has been plotted. The X_c values deduced from the curves have been plotted in the upper left corner of the graph.

The melting peak positions are close for the three samples (ca. 178°C). The classical interpretation concerning the lamellar thickness using the Gibbs–Thomson equation [eq. (3)] is not relevant here because the crystal surface energy and even melting enthalpy could be different for POM-CM, POM-N, and POM-HVC. However, the lamellar thickness should be close for the three materials.

POM-N and POM-HVC exhibit a very high X_c value (close to 90%) in comparison with POM-CM (66%). POM-HVC stays as crystalline as POM-N, confirming that the nascent powder has not undergone significant melting during HVC. Conventional processes such as compression molding, involving a melting stage, lead to a significantly lower crystallinity.

Density measurements

The density can vary with the crystallinity degree and porosity, but DSC experiments have shown that every sample processed by HVC has approximately the same crystallinity degree. Then, the density is an indicator of the pore presence.

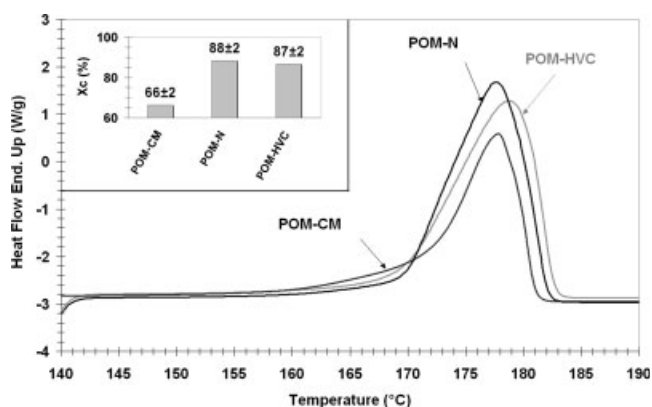


Figure 2 Crystallinity degrees from DSC experiments.

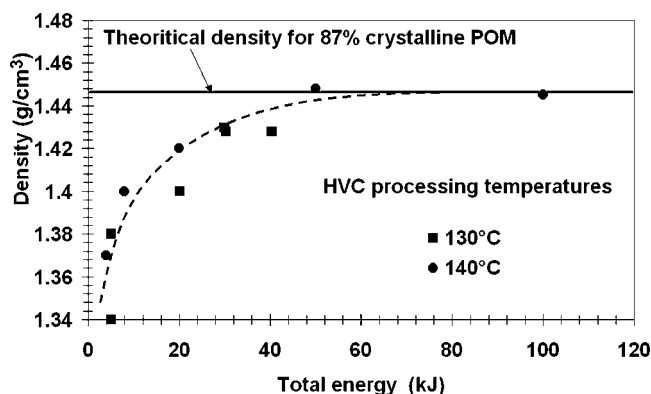


Figure 3 Density of the HVC samples versus the total energy.

The densities have been plotted versus the total energy for two processing temperatures (Fig. 3). From the graph, the density increases with the total compaction energy until a limit is reached. This limit is consistent with the theoretical value of 1.446, which was calculated for a completely dense sample with an X_c value of 87%. Full densification of the sample occurs only above 50 kJ, and below this energy, there is remaining porosity.

It is worth noting that the process temperature has no significant influence on the density evolution versus the total energy.

Small-strain mechanical characterization (DMA)

Low-HVC samples are not machinable (it seems that the particles are not bonded together), whereas medium- and high-HVC ones can be cut into small strips for DMA experiments.

The shear modulus and loss angle obtained from DMA experiments for both POM-HVC and POM-CM have been plotted versus the temperature in Figure 4.

First, it is observed that above the glass-transition temperature, POM-HVC is 50–100% stiffer than POM-CM! To explain this result, it is necessary to

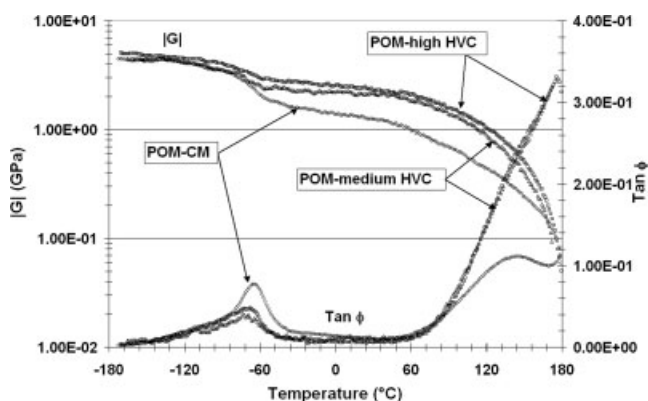


Figure 4 Shear modulus ($|G|$) and loss angle ($\tan \phi$) from the DMA experiments.

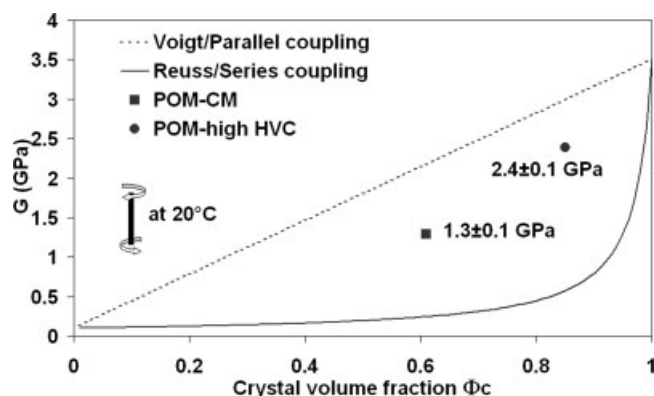


Figure 5 Position of the experimental shear modulus (G) at 20°C.

recall that semicrystalline polymers can be seen as nanocomposite materials composed of a crystal stiff phase and an amorphous soft phase.¹⁷ Above the glass-transition temperature, the crystal phase is 10^2 – 10^4 times stiffer than the amorphous phase.^{17,18} Therefore, according to mixing rules, the crystallinity governs the macroscopic stiffness of semicrystalline polymers.

Classical Voigt (parallel) and Reuss (series) mixing rules, representing the shear modulus upper and lower bounds, allow a quantitative analysis to be conducted. The corresponding equations are¹⁷

$$G_{\text{Voigt/Parallel}} = G_C \cdot \Phi_C + G_A \cdot (1 - \Phi_C) \quad (4)$$

$$G_{\text{Reuss/Series}} = \frac{1}{\frac{(1-\Phi_C)}{G_A} + \frac{\Phi_C}{G_C}} \quad (5)$$

where G_C , G_A , and Φ_C are the crystal-phase shear modulus, amorphous-phase shear modulus, and crystal volume fraction, respectively.

We have plotted in Figure 5 experimental values of the shear modulus and theoretical lower and upper bounds versus the crystal volume fraction. The following values for the crystal and amorphous shear modulus, estimated from a previous piece of work,¹² have been used: 3.5 and 0.1 GPa, respectively. This graph shows that the high modulus of POM-HVC is consistent with the crystallinity degree measured by DSC.

Concerning the loss-angle curves, the relaxation peak associated with the glass transition (ca. -70°C) is less pronounced for HVC materials than for molded ones. This transition peak amplitude is generally related to the amount of the amorphous phase; thus, this observation is consistent with DSC measurements.

Following a similar analysis, we notice that the relaxation peak around 120°C , generally associated with crystal defect mobility,¹⁴ is more pronounced

for POM-HVC because of a more significant crystallinity degree and/or more crystal defects.

Mechanical characterization until rupture (bending tests)

To study POM-HVC rupture behavior, bending tests at 20°C have been conducted. Stress–strain curves have been plotted in Figure 6 for POM-CM, medium-energy high-velocity-compaction polyoxymethylene (POM-medium HVC), and high-energy high-velocity-compaction polyoxymethylene (POM-high HVC).

One can notice that the gain in the modulus observed in DMA is confirmed. Young's modulus of POM-high HVC is about 5 GPa, whereas for POM-CM, it is only 3 GPa.

However, brittle behavior is observed for POM-HVC, with rupture occurring between 0.5 and 1% deformation, whereas POM-CM is ductile. It is obvious that brittleness is a shortcoming for POM-HVC. Nevertheless, the elastic limit stress of POM-high HVC (the maximum stress in the linear domain is interpreted as an elastic limit) reaches that of POM-CM (~ 40 MPa; see the tangent plot in Fig. 6). To compare the fracture stress values, as the stress calculation from ASTM D 790¹⁶ is not valid at large strains, information from tensile tests can be used. POM-CM fracture occurs above a 30% strain at approximately 70 MPa (nominal stress) under a tensile test,⁷ whereas the POM-high HVC fracture stress is about 50 MPa.

Influence of the process parameters on the mechanical properties

As shown in Figures 4 and 6, the HVC process parameters influence the final mechanical properties. To study this influence, Young's moduli obtained from bending tests have been plotted versus the total energy for the three HVC processing temperatures

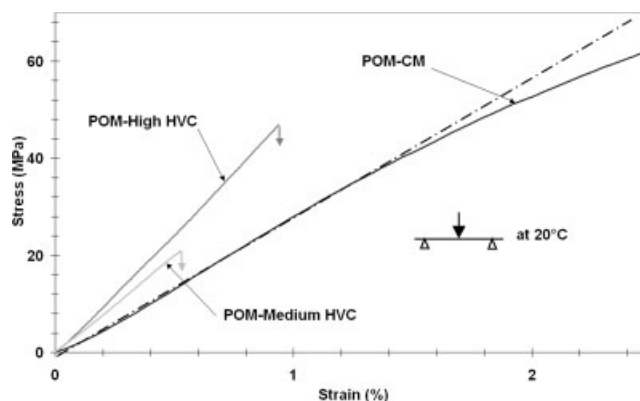


Figure 6 Stress–strain curves from three-point-bending tests at 20°C.

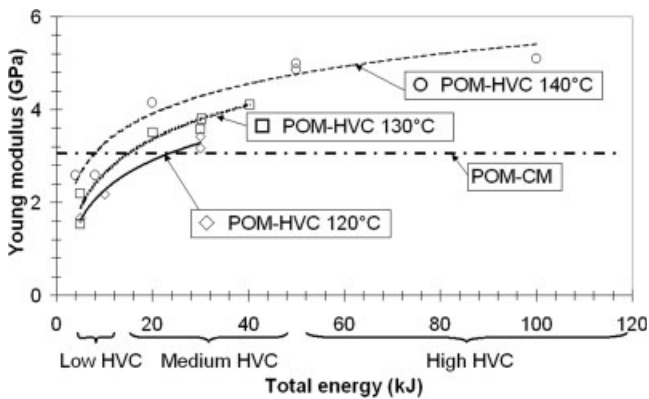


Figure 7 Young's modulus from bending tests versus the process temperature and total energy.

(120, 130, and 140°C) in Figure 7. The POM-CM value has been added for comparison. One can notice that Young's modulus increases with the total energy until a maximum value. This modulus increase is more pronounced for high processing temperatures, and for a processing temperature of 140°C, the exceptional value of 5 GPa is reached. As previously mentioned, this high stiffness is due to a high degree of crystallinity. The weak sintering of low- and medium-HVC samples, revealed by remaining pores, leads to low Young's moduli.

Likewise, the values of the fracture stress have been plotted versus the total energy for the three processing temperatures (Fig. 8). The fracture stress can be calculated from bending tests as POM-HVC breaks at small strains. This is not the case for POM-CM, and this is why the fracture stress of POM-CM has been taken from the *Polymer Handbook*.⁷ As for Young's modulus, the fracture stress increases with the energy until 50 MPa for POM-high HVC. Regarding the temperature influence, one can notice that the mechanical improvement with the total energy is more significant at a high processing temperature. However, it has not been possible to fur-

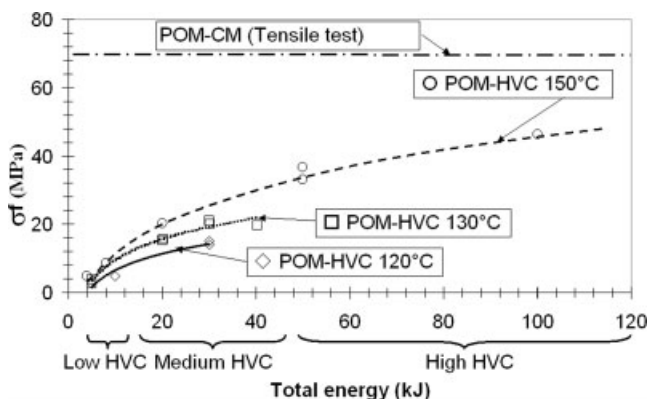


Figure 8 Fracture stress (σ_f) from bending tests versus the process temperature and total energy.

ther improve the fracture stress because polymer degradation appears at a higher temperature.

To summarize, for high impact energy, POM-HVC reaches a higher stiffness than POM-CM because of the high crystallinity of the nascent powder. The fracture stress rises with the impact energy and temperature until 50 MPa, but it is still under the POM-CM value, and for any HVC conditions, POM-HVC is brittle.

In the next section, we attempt to understand the brittleness and propose a sintering mechanism based on LVSEM observations and compressive tests.

DISCUSSION

Is POM-HVC brittleness due to weak interfaces?

To determine the origin of the brittle behavior of HVC materials, first some LVSEM was performed on bending test fracture surfaces.

As observed in Figure 9, medium-energy HVC samples exhibit an interparticle failure: fracture has occurred by particle decohesion, likely because of weak sintering. In Figure 10, at a higher magnification, cavities of several micrometers (microporosity), separated by fibrils, can be observed at the particle interfaces. First of all, the presence of fibrils proves that some links between particles have been created during HVC. It is assumed that fibrils have been formed by the stretching of local links. The first hypothesis would be to propose that fibrils have been formed during bending sample fracture, but additional LVSEM observations of the surface of nondeformed samples also show fibrils. Moreover, the presence of interface microporosity is consistent with density measurements (Fig. 3) showing that POM-medium HVC has not reached full density. Actually, it is assumed that fibrils originate in particle thermal

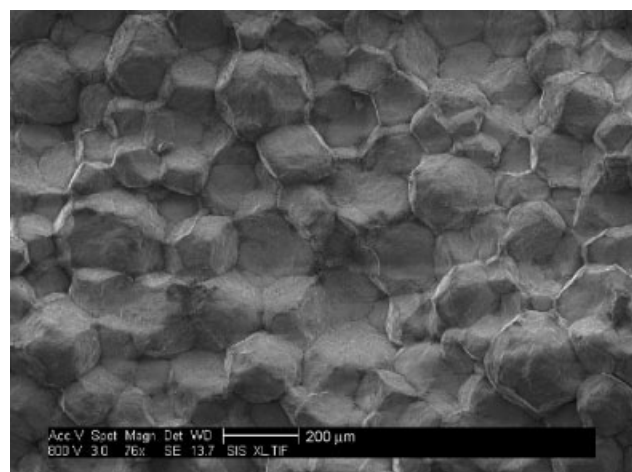


Figure 9 LVSEM fracture surface observation: interparticle failure of POM-medium HVC.

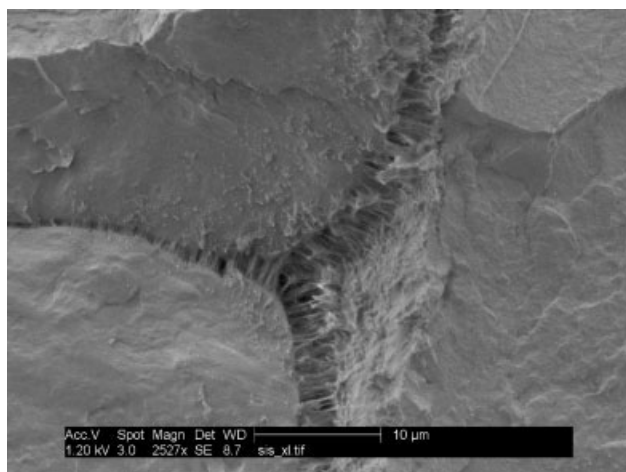


Figure 10 LVSEM fracture surface observation: fibrils and microporosity at particle interfaces of POM-medium HVC.

contraction during cooling. This hypothesis would lead to interfaces around 1 μm in size (thermal contraction coefficient: $\sim 10^{-4}/\text{K}^7$), which is of the same order of magnitude as interfaces observed in micrographs. In addition, viscoelastic recovery after ejection could also cause particle contraction.

Consequently, brittleness originates in bad particle bonding and resulting weak interfaces (fibrils and microporosity).

On the contrary, high-energy HVC samples exhibit a mainly transparticle failure, proving that for these samples there are strong links between particles (Fig. 11). Similarly to POM-medium HVC, POM-high HVC has been observed at higher magnifications. No microporosity is noticeable at particle interfaces (Fig. 11). The absence of microporosity is confirmed by density measurements (Fig. 3): the theoretical nominal density has been reached. However, the interface is still visible, forming a step between two particles failed in a brittle manner, proving that it is a weaker zone, probably with remaining interfacial defects resulting from imperfect sintering.

The visual aspect of the material confirms those observations. At low and medium HVC, the material is opaque and white: persisting cavities between particles scatter light. This phenomenon is the same as the often observed whitening of polymers during cavitations due to plastic deformation. As cavities scatter light, their sizes are expected to be of the same order of magnitude as the wavelength of light (400–700 nm),¹⁹ and this is consistent with LVSEM pore observations (Fig. 10). On the contrary, POM-high HVC has a more transparent aspect, similar to the molded one, which reveals an absence of pores able to scatter light.

In summary, even with good sintering proved by the absence of microporosity at the particle interfaces and transparticle failure, POM-HVC is brittle.

Is the brittleness of POM-HVC intrinsic?

Concerning POM-high HVC, as it is obvious that sintering is good, it is thought that brittleness cannot originate entirely in possible minor interfacial defects.

The sharp aspect of broken particles on a fracture surface (Fig. 11) leads us to suspect that powder particles are brittle at room temperature.

To confirm this, nascent particles were crushed at room temperature and then observed under LVSEM. The micrograph (Fig. 12) reveals that the particles are really brittle: one can see a significant crack with a sharp broken surface. The same test was conducted at 130°C, above the α_c transition, to enhance crystal deformation. At 130°C, the nascent POM particles are ductile: they exhibit high deformation without breaking (Fig. 13).

As a result, it is interesting to distinguish the intrinsic material brittleness from the extrinsic brittleness due to imperfect particle bonding.

To understand the intrinsic brittleness, it is important to keep in mind the mechanisms involved in the

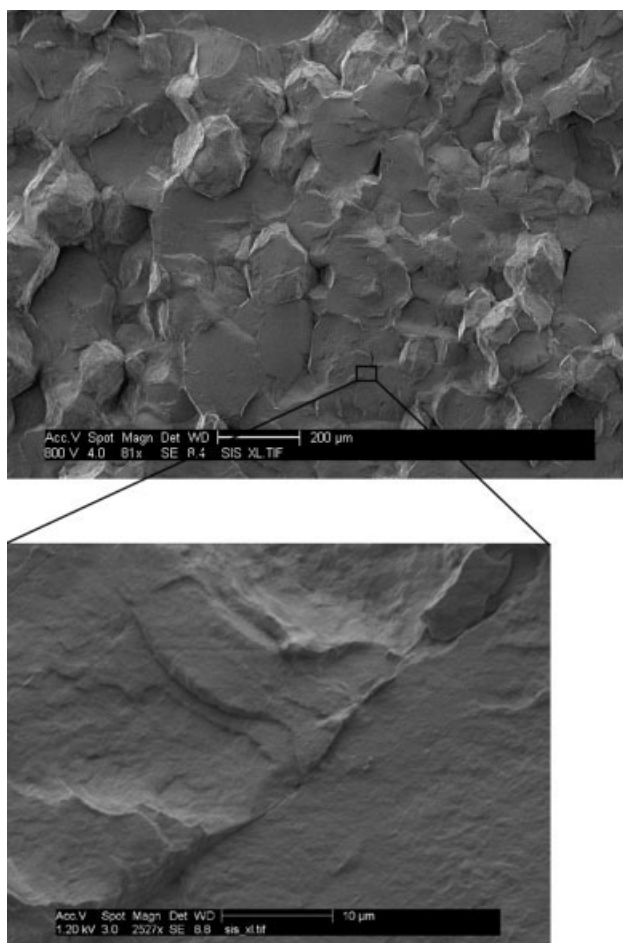


Figure 11 LVSEM room-temperature fracture surface observation: POM-high HVC.



Figure 12 LVSEM observation: fractured nascent POM particle crushed at room temperature.

plasticity of semicrystalline polymers. The generally admitted model proposes that an amorphous phase deforms first until the stress is sufficient to shear and then fragment crystal lamellae.²⁰ If the stress required to shear plastically crystal lamellae cannot be transmitted by molecular connections between the crystallites (formed by the so-called tie molecules²¹), fracture occurs by amorphous chain slippage or scission, and the material is brittle.²²

It follows that the crystallites' morphology and crystallization conditions influence the mechanical behavior of the polymer. Indeed, the yield stress varies with the polymer crystal-phase microstructure (lamellar thickness and crystal perfection), and a high yield stress will not allow ductility development before breaking.^{22–24} Polymer crystallization conditions influence also the ductility through the variation of the tie-molecule concentration: a small

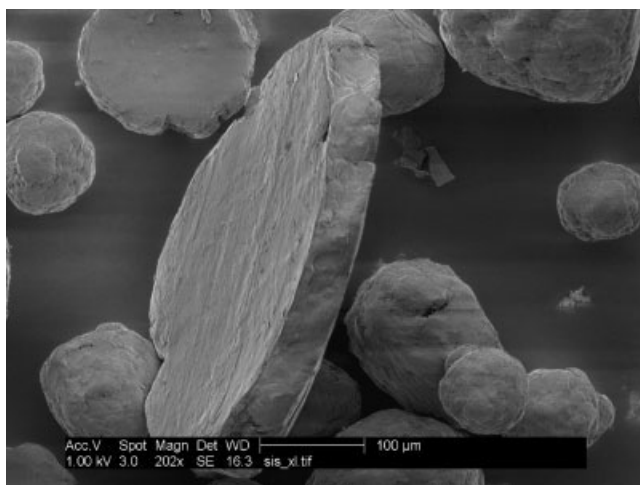


Figure 13 LVSEM observation: highly deformed nascent POM particle crushed at 130°C.

number of tie molecules will not transmit enough stress to shear and fragment lamellae and will lead to a brittle material.²²

DSC experiments (Fig. 2) have shown that the nascent powder does not undergo significant melting during HVC. Thus, the crystal-phase morphology and tie-molecule concentration of the nascent powder are mainly preserved after HVC. Unfortunately, data are missing in the literature concerning nascent POM morphology. Despite the lack of knowledge, it is conceivable that nascent POM exhibits a more perfect crystal phase and/or thicker lamellae leading to a higher yield stress in comparison with injected POM. It is also conceivable to think that crystallization during polymerization does not favor the formation of tie molecules.

To validate our assumptions on the origin of the intrinsic brittleness, compressive tests were performed. In the compressive stress state, the effect of material flaws is less pronounced (compression tends to close nascent cracks), and the fracture stress is higher, favoring plasticity.

Compressive stress–strain curves at 20°C have been plotted in Figure 14. One can see that POM-HVC is still brittle, but with a very high fracture stress. It is noted that the plasticity of POM-high HVC initiates around 80 MPa, whereas that of POM-CM initiates at 30 MPa: it is obvious that the yield stress of POM-HVC is significantly higher than that of POM-CM. It validates the previous analysis assuming that POM-HVC is intrinsically brittle because of a high yield stress originating in the particular nascent crystal structure.

Mechanical testing at 130°C was then performed: at this temperature, the particles are ductile, and thus the influence of the intrinsic brittleness due to the nascent crystal structure is reduced.

Figure 15 shows the compressive stress–strain curves at 130°C. High strains have been reached, proving that the intrinsic brittleness has a significant

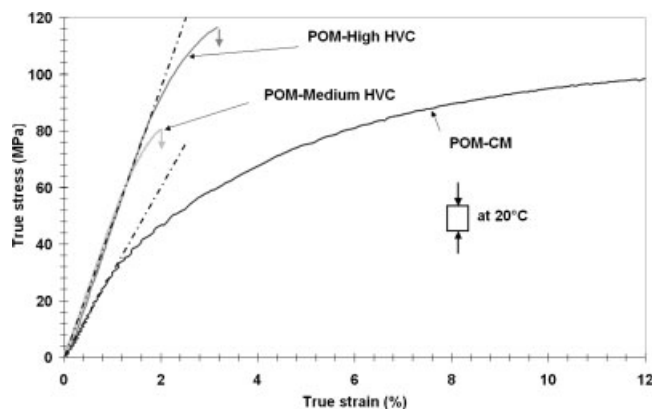


Figure 14 Stress–strain curves from compressive tests at 20°C.

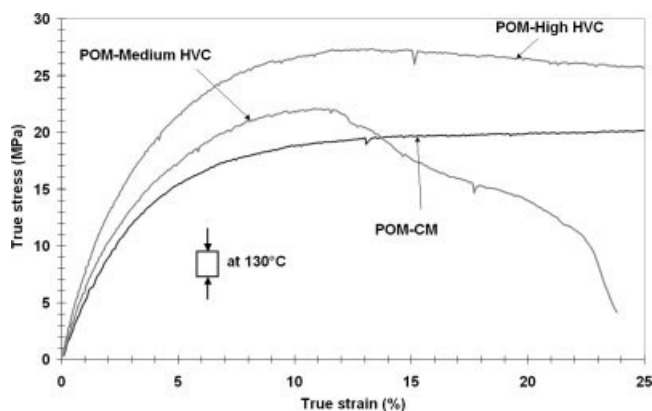


Figure 15 Stress–strain curves from compressive tests at 130°C.

influence at 20°C. In addition, the high yield stress of POM-high HVC is confirmed.

Bending tests carried out at 130°C (Fig. 16) revealed that POM-HVC is still brittle, even if the fracture strain is improved in comparison with room-temperature testing. Yielding has not been reached as in the 130°C compressive tests. This tensile/compressive dissymmetry at 130°C can be explained mainly by the presence of remaining interfacial defects, which favor cracking in a tensile stress state.

The analysis concerning brittleness at 20°C can be summarized as follows:

- Low-energy high-velocity-compaction polyoxymethylene (POM-low HVC) and POM-medium HVC have brittle behavior because of poor particle bonding and resulting weak interfaces formed of fibrils and microcavities.
- Similar interface microporosity has not been found on POM-high HVC. In addition, POM-high HVC exhibits a transparticle failure at 20°C; thus, the brittleness origin is not clear. On the

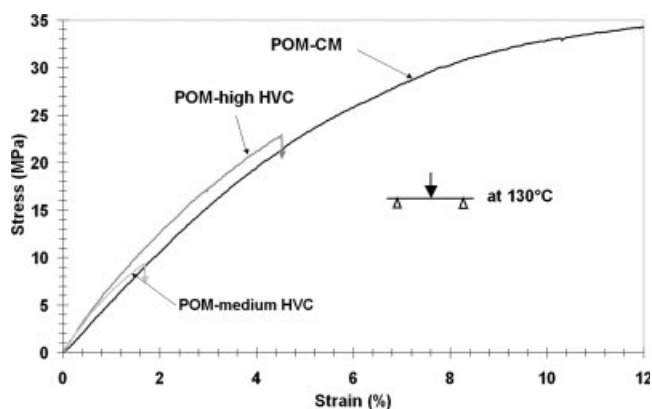


Figure 16 Stress–strain curves from three-point-bending tests at 130°C.

one hand, there is strong evidence that the powder is intrinsically brittle because of a high yield stress induced by a particular crystal structure. On the other hand, interfacial defects can remain, as interfaces are still visible on fractographs and the material is still brittle at 130°C.

In conclusion, it should be possible to improve the fracture stress by better sintering, but it is believed that even a well-sintered material with no weak interfaces will stay brittle at room temperature because of the intrinsic brittleness of the powder.

Sintering mechanism

Good mechanical properties and transparticle failure prove that strong links between particles have been created during high-energy HVC. Fibrils between particles on POM-medium HVC (Fig. 10) are not visible on POM-high HVC samples (Fig. 11). In this last case, local links appear to be strong enough to resist the stress imposed by viscoelastic and/or thermal contraction of the particles. As a result, no fibrillation or cavity formation occurs during the HVC process or subsequent cooling, and this proves a strong link existence.

Some studies on welding²⁵ and hot compaction of fibers²⁶ have reported that local melting followed by recrystallization can bond polymer interfaces. Furthermore, a study on POM static hot compaction has shown that partial melting is necessary to achieve the welding of powder particles.¹²

Regarding the HVC process, it is also assumed that welding occurs via fusion/recrystallization. More precisely, it is thought that self-heating in the sample, caused by friction between the particles, provokes melting of their surface and then their subsequent welding by recrystallization during the cooling (Fig. 17).

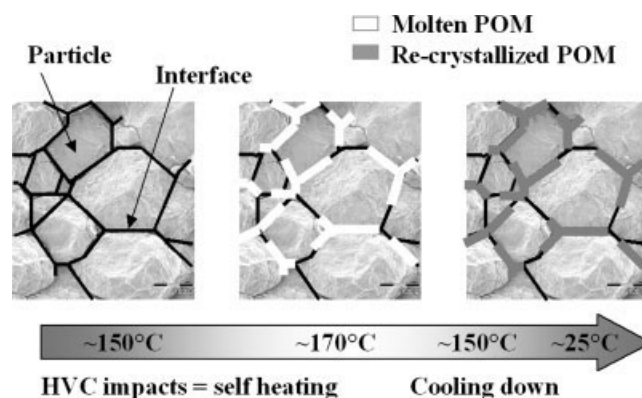


Figure 17 Schematic representation of the sintering mechanism.

CONCLUSIONS

The new HVC process of a polymer powder, based on several high-energy impacts, gives encouraging results for POM. Compared with conventional polymer processing, HVC presents several advantages. First, it allows the production of parts with no significant shrinkage or cavities, even with a large thickness. Moreover, because of the preserved high crystallinity of the nascent POM powder, POM-HVC exhibits high stiffness.

On the other hand, the intrinsic brittleness of nascent POM, due to a particular crystal morphology, is likely to induce the brittleness of POM-HVC at room temperature. However, POM-HVC is easily machinable and completely elastic until its fracture around 50 MPa in the tensile stress state and around 110 MPa in the compressive stress state.

Despite its brittleness, POM-HVC has a sufficiently high fracture stress to be considered for certain applications, such as parts loaded in compression under the elastic limit. Shapes must also be simple to avoid additional machining. Seals are a satisfactory example of a possible application.

As material imperfections due to the HVC process (extrinsic brittleness) are not the only cause of brittleness at 20°C, we are optimistic regarding the extension of the process to other materials for which the nascent powder would be ductile. In particular, it would be interesting to extend HVC to non-melt-processable, high-molecular-weight polymers. Concerning POM-HVC, the improvement of the ductility will be attempted with more ductile POM powders. Another option would be to improve the chemical stability of nascent POM powder to be able to melt a significant part of the powder during HVC; thus, the fraction of the nascent crystalline structure likely responsible for the brittleness would be reduced. High-molecular-weight and semicrystalline polymers involving processing difficulties (degradation and/or cavity formation) should be easier to process with the HVC process. The improvement of the mechanical, tribological, and electrical properties may be possible because of the addition of large quantities of fillers allowed by HVC and the use of nascent, highly crystalline polymer powders.

References

1. Wilkinson, A. N.; Ryan, A. J. *Polymer Processing and Structure Development*; Kluwer Academic: Dordrecht, 1998.
2. German, R. M. *Powder Metallurgy Science*; Metal Powder Industries Federation: Princeton, NJ, 1984.
3. Andena, L.; Rink, M. *Polym Eng Sci* 2004, 44, 1368.
4. Hambir, S. S.; Jog, J. P.; Nadkarni, V. M. *Polym Eng Sci* 1994, 34, 1065.
5. Paransis, N. C.; Ramani, K. *J Mater Sci: Mater Med* 1998, 9, 165.
6. Kelly, J. M. *J Macromol Sci Polym Rev* 2002, 42, 355.
7. Brandrup, J.; Immergut, E. H.; Bloch, D. R.; Gruckle, E. A. *Polymer Handbook*; Wiley: New York, 1999.
8. Wunderlich, B. *Macromolecular Physics*; Academic: New York, 1980.
9. *General Design Principles—Module I*; DuPont Engineering Polymers: Le Grand Saconnex, Switzerland, 2006.
10. Hama, H.; Tashiro, K. *Polymer* 2003, 44, 2159.
11. Lazzarotto, L.; Doré, F.; Allibert, C. H.; Doremus, P.; Goeuriot, P.; Lame, O. In *Proceedings of the 4th International Conference on Science, Technology and Applications of Sintering*, Grenoble, France, 2005; Bouvard, D., Ed.; Institut National Polytechnique de Grenoble, Grenoble, France.
12. Al Jebawi, K.; Sixou, B.; Seguela, R.; Vigier, G.; Chervin, C. *J Appl Polym Sci* 2006, 102, 1274.
13. Bershtein, V. A.; Egorova, L. M.; Egorov, V. M. *Thermochim Acta* 2002, 391, 227.
14. Johnson, M. B. *Investigations of the Processing–Structure–Property Relationships of Selected Semicrystalline Polymers*; Faculty of the Virginia Polytechnic Institute: Blacksburg, Virginia, 2000.
15. Wunderlich, B. *J Therm Anal* 1996, 46, 643.
16. ASTM Standard D790: Test Method for the Flexural Properties of Unreinforced and Reinforced Plastics and Electrical Insulation Materials; *Annual Book of ASTM Standards*; American Society for Testing and Materials: Philadelphia, 1999; p 269.
17. Ward, I. M.; Sweeney, J. *Mechanical Properties of Solid Polymers*; Wiley: London, 2004.
18. Boyd, R. H. *Polym Eng Sci* 1979, 19, 1010.
19. Quatravaux, T.; Elkun, S.; G'Sell, C.; Cangemi, L.; Meimon, Y. *J Polym Sci Part B: Polym Phys* 2002, 40, 2516.
20. Schultz, J. M. *Polymer Materials Science*; Prentice Hall: Englewood Cliffs, NJ, 1974.
21. Seguela, R. *J Polym Sci Part B: Polym Phys* 2005, 43, 1729.
22. Brown, N.; Ward, I. M. *J Mater Sci* 1983, 18, 1405.
23. Schrauwen, B. A. G.; Jansen, R. P. M.; Govaert, L. E.; Meijer, H. E. H. *Macromolecules* 2004, 37, 6069.
24. Gaucher-Miri, V.; Seguela, R. *Macromolecules* 1997, 30, 1158.
25. Bonten, C.; Schmachtenberg, E. *Polym Eng Sci* 2001, 41, 475.
26. Ward, I. M.; Hine, P. J. *Polymer* 2004, 45, 1413.